Seismic Attenuation for Reservoir Characterization

DE-FC26-01BC15356

Quarterly Report
July 1, 2003 to September 30, 2003

Issued October, 2003

Contributors

Dr. Joel Walls*

Dr. M. T. Taner*

Naum Derzhi*

Dr. Gary Mavko**

Dr. Jack Dvorkin**

*Principal Contractor:

Rock Solid Images

2600 S. Gessner Suite 650

Houston, TX, 77036

**Subcontractor:

Petrophysical Consulting Inc.

730 Glenmere Way

Emerald Hills, CA, 94062

Disclaimer

Abstract

In this report we will show the fundamental concepts of two different methods to compute seismic energy absorption. The first methods gives and absolute value of Q and is based on computation with minimum phase operators. The second method gives a relative energy loss compared to a background trend. This method is a rapid, qualitative indicator of anomalous absorption and can be combined with other attributes such as band limited acoustic impedance to indicate areas of likely gas saturation.

Contents

Experimental

No experimental work is reported. Data shown are from commercial well logs and seismic data contractors.

Results and Discussion

Section 1: Q Computation with Minimum Phase Operators

Introduction:

Last year we experimented with several methods to estimate Q from seismic data. Spectral division, the main tool for Q computation, still proves to be the best method. We have used the Gabor-Morlet Joint Time-Frequency decomposition to estimate the local spectra. This gives fairly good results with synthetic data. The biggest problem was the choice of the band-width for Q estimation. The next most interesting method was spectral estimation by the minimum phase inverse operators. This method proved to be very flexible and robust. It was flexible, because by changing the order of the polynomial division, one could compute either the Q computation or Q compensation operator. We have decided to implement this method for computing Q from 3-D seismic data. This report will cover the technical details of Q computation with minimum phase operators. All of the methods gave inhomogeneous results (it appeared noisy, because results did not track events), hence we had to consider some spatial consistency checking and proper smoothing.

General Assumptions and Problems:

There are a number of methods proposed for Q computation. Most of the methods give poor to fair estimates of Q. The most common problem is Q estimates are very noisy or spatially very inconsistent. Q values, being a bedding attribute, are similar to the interval velocities. Their effects are accumulative, hence they can be measured by differentiation, which sets a condition conducive for additional noise generation. Like velocities, we could estimate average, RMS or interval Q values. However, the most interesting is the inter-bed Q estimate. Here we come up against the resolution problem: "How thin a bed can we resolve?" Velocities are measured from picked events. Attenuation on the other hand, is measured from spectral signatures, as well as picked events. Therefore, we are not bound to track events and compute spectral variations over closely spaced windows. However, the closer the windows, the smaller the Q effects, and hence we get noisier estimates. It means that we have to consider some noise reduction procedures.

One of the common methods is to incorporate areal estimates. This is based on the assumption that Q does not vary abruptly from trace to trace, but it may vary from layer to layer. This assumption implies Q values should be more consistent along bedding, hence we can put some restriction or initial condition in our computation. In the present method we have included an edge preserving smoothing process prior to the Q computation. This helped to some degree. After smoothing, we have scanned the data to determine the principal slopes of events. Summing adjacent traces along the principal slopes formed average traces. First experiments were run by computing Q from the scanned average traces. Results, while improved over previous trials, still showed excessive scattering of Q values. After Q computation, we used the computed slopes as the direction of data to be included in the spatial smoothing. Results looked too blocky. The second method was to average autocorrelation functions. As in the edge preserving smoothing, we have averaged autocorrelations of the trace at the center and its eight neighbors. Computations showed considerably better stability and produced higher resolution of Q values. While there was some scatter, consistencies along bedding became discernable.

The most accurate method of Q computation is the spectral ratio. However, before the ratio is computed, we have to make sure the spectra do not have any zero or negative values. These erroneous values are the result of poorly computed autocorrelation functions. Gabor-Morlet joint time-frequency analysis (JTFA) provides us with instantaneous amplitude and phase spectra. This can be used for ratio computation. Our JTFA experiments with synthetic data did give good results. Only problem is, due to noisy background, we cannot use the full spectral band. We have to determine the zone with best signal to noise ratio. We can determine this band in the minimum phase method, which I will describe below.

Method:

The program examines 3 cross-lines at one time. This is used in the edge preserving smoothing section routine. The main computational steps are as follows;

1) Read data, in the beginning accumulate at least 2 cross lines, otherwise work with 3 cross lines at a time. During the process, output one cross line and read a new one recursively.

2) Apply edge-preserving smoothing to one cross line,

3) Apply dip-scan to generate dip optimized traces and event dips,

4) Apply two different method of autocorrelation computation;

a) Autocorrelation was computed from dip optimized traces. This did not work well.

b) Autocorrelations of central trace and eight of its neighbors were averaged. This produced stable results.

5) Compute Q values between zero crossing more that 3 samples apart, (computational details will be described in the next section.)

6) Pick Q values along the event dips using a Gaussian weight to compute sample by sample weighted Q average.

7) Output Q values one cross line at a time, read new one in until all lines are done.

Mathematical Detail:

Q computation is performed by synthetic division of minimum phase inverse wavelets computed over two time zones. The minimum phase wavelets do not have any zeros on the unit circle. They can be very short, hence their autocorrelation can also be very short. This will improve the time resolution.

1) Select a short operator length, say 60 to 80 milliseconds,

2) Autocorrelation window length could be about 200 to 400 milliseconds.

3) For each window, find the nearest zero crossing, and place the beginning of autocorrelation window to the zero crossing. This will give a stable estimate.

4) Compute autocorrelation at each zero crossing and compute minimum phase inverse operator from each autocorrelation by the Wiener-Levinson algorithm. (This was modified in the second method. Autocorrelations of the center trace and its eight neighbors are summed to get a better and more stable autocorrelation estimate.)

5) For each adjacent (in time) pair of operators, determine the spectral ratio computation band. This band must contain best signal to noise ratio between the two spectra involved in the computation.

Compute inverse of deeper operator and compute its Fourier transform. This will give the estimate of the deeper wavelet amplitude spectrum. The deeper wavelet has been through more of the absorptive medium than the shallower wavelet, hence it should have the narrower band width. We determine the main peak of the spectrum and the ½ power point on either side of the main peak. Since the operator was very short, our spectrum will be smooth, reflecting mainly the seismic wavelet. Therefore ½ maximum amplitude band limits will be best signal to noise zone for spectral ratio computation.

Unfortunately, very short minimum phase inverse operators spectra had considerable amount of power in low frequency region that produce the peaks at very low frequencies

with very narrow band limits. This method was abandoned in favor of the method used after spectral division, as explained below.

6) Compute synthetic (polynomial) division between two adjacent operators, with the shallow operator on the numerator and deeper one in the denominator. The quotient will be the Q operator.

7) Compute Fourier transform of the quotient and determine its log amplitude spectrum.

8) Line fit to the log spectrum over the band width determined previously. The slope of the fitted line will be the desired Q value. The line fit should contain some weighting to prevent adverse effects of outliers. We used number of narrow band limited areas over the whole spectra and computed Q values for each zone, then used the most consistent Q value as the final result.

In subsequent tests we have observed that averaging autocorrelations along bedding is better than trace averaging. This implies that we can apply some weighted smoothing along bedding that minimize the scatter with least damage to the Q structure.

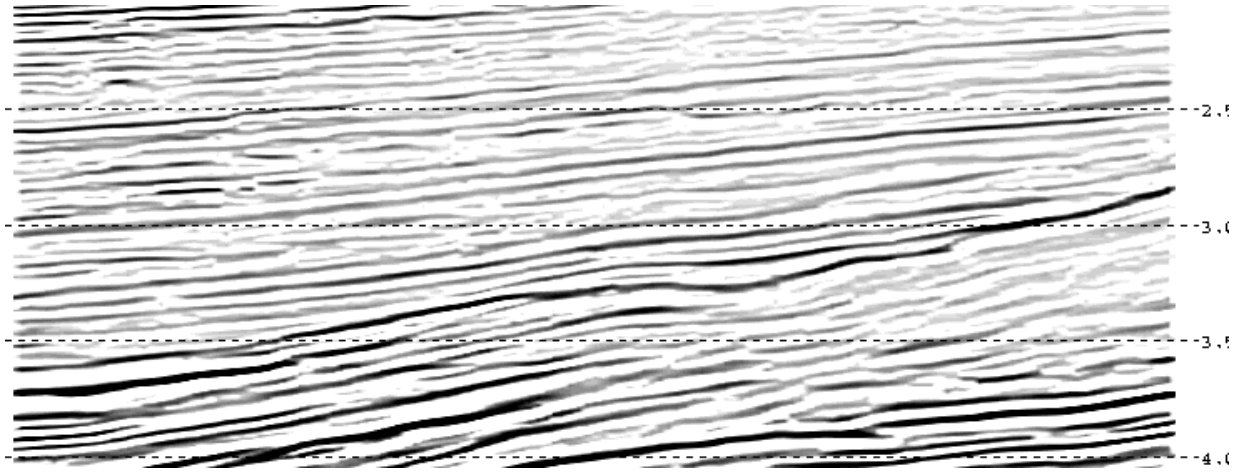

Figure 1: A portion of a cross line input to the computation program.

Figure 1 shows a portion of the line used as a test line for Q computation procedure described in this report. We have generated sections from various stages of processing to show the effects of each processing step.

The input data is first passed through the edge preserving smoothing in order to improve the signal to noise ratio and improve the lateral continuity. By improved lateral continuity we expect to compute more consistent Q values along the events.

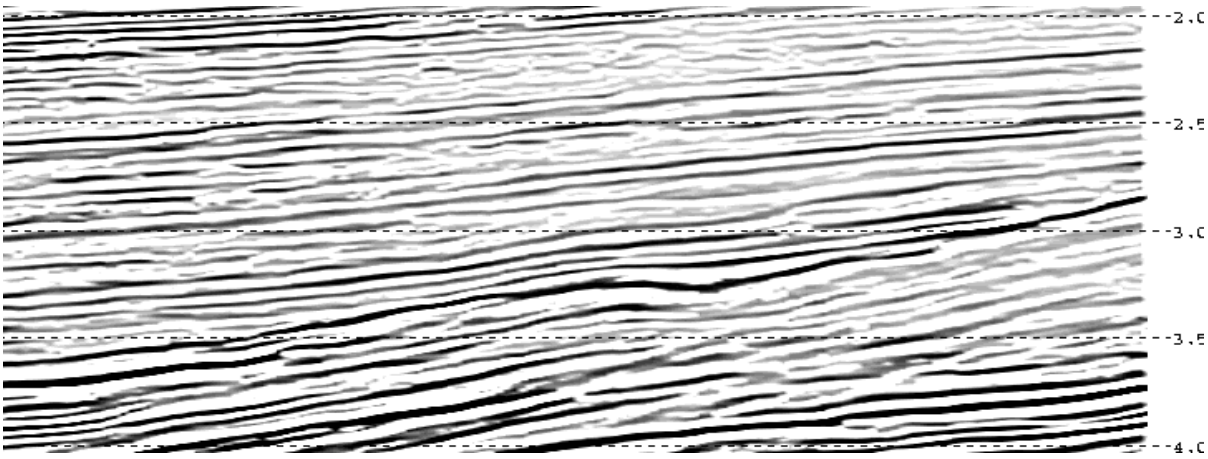

Figure 2: Input data after edge preserving smoothing.

Edge preserving smoothing, shown in Figure 2 is a fast and effective process. It improves lateral continuity while preserving discontinuities such as faults and structural or stratigraphic terminations. Comparing Figure 2 with Figure 1 help visualize the degree of improvement of noise suppression.

We assume that computed Q values should be more continuous along the bedding and may change more rapidly from one bed to the next in depth direction. In order to follow the bedding we need to have the bed dips. This is computed by the dip scan routine.

Figure 3: Result of Dip scanning and lateral continuity enhancement.

The dip scan routine considers an odd number of traces, as requested by the user, and scans linear dips around each trace location. It uses a user specified window length, and computes continuous semblance in time for each dip. It detects the dip of maximum semblance and generates data in that window by summing traces along maximum semblance dip. The maximum semblance, corresponding dip and optimum trace are

saved for the final output. Figure 3 shows the output from dip scanning process. The dips computed by this routine show the direction of bedding, which will be used in lateral smoothing of the computed Q values.

Figure 4 shows the computed Q values from averaged autocorrelation functions. We used three adjacent in-lines. Thus, for each trace in the center there were 8 neighboring traces, hence we could average 9 autocorrelation functions. Dips inline and crossline directions gave the estimated positions of the zero crossings on the neighboring traces. Hence autocorrelations were taking at relatively the same events along the structural dip directions. .

Figure 4 shows clearly that most Q values were computed within the acceptable range. This was also indicated by the stable autocorrelation printout of the program. We still have considerable amount of variable Q values, but there are definite similarities along the bedding patterns. This will be suitable to smoothing application following the bed structure. The warmer colors indicate lower Q values, and cooler colors indicate higher Q values. Dark blue colors are representing Q values around 120, and red values are around 15.

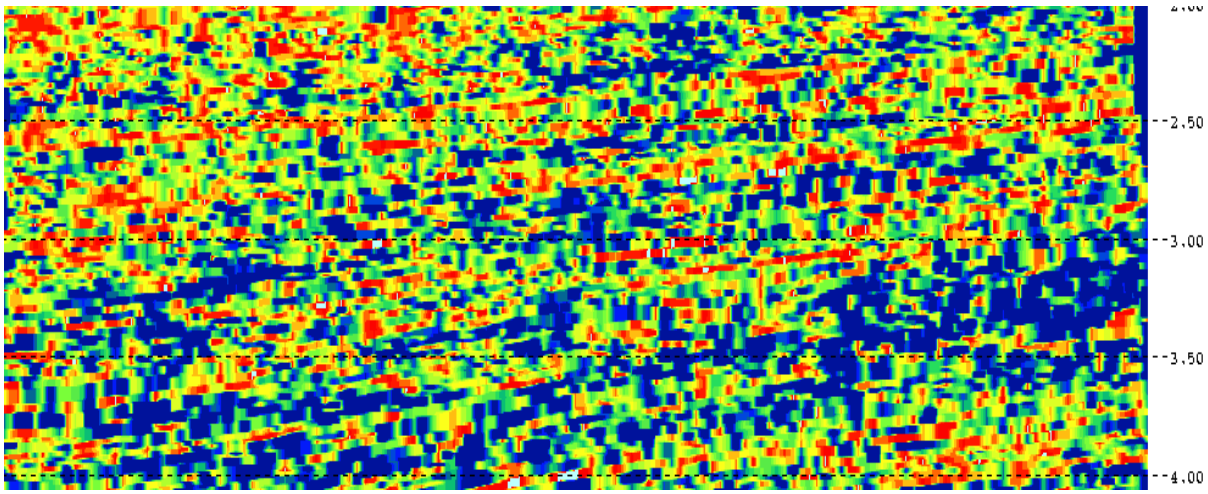

Figure 4: Q computation using the average autocorrelation functions of neighboring traces.

In order to reduce the noise and recover some continuity, we apply lateral continuity enhancing smoothing. In this process, a number of adjacent samples along the bed direction are used. If the center trace is a valid Q number, we sum all valid Q numbers weighted by a Gaussian filter and determine the Gaussian average, and replace the center value with the average.

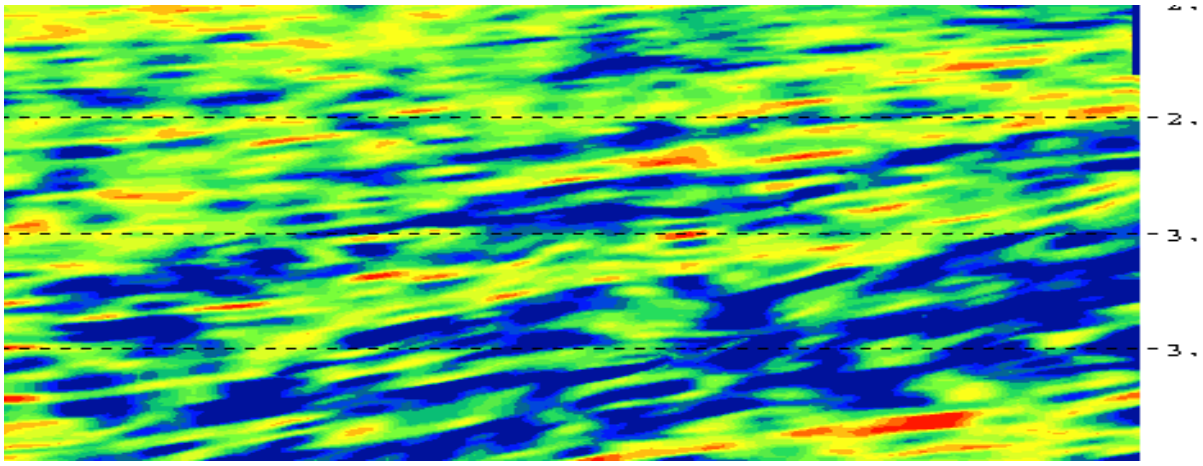

Figure 5: Spatial averaging applied to the Q computation shown on figure 4. Smoothing along the structural dip direction is clearly discernable.

If the center value is invalid (like Q = 300), then we look at the number of valid and invalid samples around the point along the bed. If the number of invalid is the majority, then the point remains invalid. If valid Q values are majority, then Gaussian average will be the result. This way averaging is done in the direction of bedding and some invalid locations within valid computations will be eliminated.

Section 1 Conclusions

We have used two stages of lateral continuity enhancement process before Q computation. For each output location, a center trace and its eight neighboring trace autocorrelations were averaged. Resulting autocorrelation functions proved to be much more stable and gave considerably more accurate and consistent results. The Q computation method used in this experiment, minimum phase inverse operator polynomial division, is proven to be an accurate and robust method. It provides spectral division results without the danger of division by zero. Computation is fast and requires minimum user input decisions. The next test will be comparison between well log or VSP developed Q profile versus computed Q values.

Section 2: Anomalous Absorption

Introduction

During the development of Q computation, we have observed that the results are very noisy, when viewed closely. However, when viewed over a larger volume, they indicate some anomalous low or high Q zones. We know that Q is a bedding attribute, rather than an interface attribute. Therefore, our observation ability will depend on the bed thickness and the complexity of the bed interfaces. In many instances we do not need an absolute Q measurement. Instead we want a reliable indicator of absorption variability and some way to see anomalously high seismic attenuation. In this report we give computational details of one such estimation approach.

Method

The quality factor Q represents the transmission efficiency of the material. A high quality factor (Q) represents transmission of energy with high efficiency or small loss. Since we are seeking to detect low quality factor zones, we must detect higher energy loss areas. It is natural that the higher frequencies, while loosing approximately the same energy per cycle, loose more of their energy over the same travel distance. This results in shifting the spectral content of the seismic waves to lower frequencies, as well as narrowing their bandwidth. These two indicators will be used to detect anomalous zones. Another point is that the energy loss is continuous over travel distance, or seismic travel time. If all material were homogenous, we would expect the energy loss be of exponential form. Any variation of the quality factor will perturb this form. However, in general the overall loss trend will be smooth due to integration of the absorption effects over the travel distance. Any anomalously high absorption zone will perturb this smooth trend and will appear as a sharper rise in the rate of loss. Therefore, we try to detect the anomalous zones as a deviation from an overall trend.

Let f(t) represent a seismic trace and E(t) represent its envelope (Taner et al, 1979). First, the seismic trace f(t) is decomposed into Gabor sub-bands using the Gabor-Morlet decomposition; (Morlet et al, 1982, Koehler, 1983, Taner, 2001)

$$G(t,f) = \sum_{\tau} f(i-\tau).g(f,\tau) \qquad (1)$$

where ;

$$g(f,\tau) = e^{-i2\pi f\tau}.e^{-\alpha(f)\tau^2} \qquad (2)$$

Since the output is a complex trace in each sub-band, then

$$a(f,t) = \left| G(f,t) \right| \tag{3}$$

where a(f,t) represents the joint time-amplitude spectrum of the seismic trace, t = time, and f = frequency. (See figure 1)

Next, we compute the first and the second moments of the joint time frequency spectrum at each data sample. The first moment gives the mean value of the instantaneous spectrum;

$$F_{ave}(t) = \frac{\sum_f f.a(f,t)}{\sum_f \alpha(f,t)} \tag{4}$$

and the second moment is;

$$F^2_{RMS}(t) = \frac{\sum_f f^2.a(f,t)}{\sum_f \alpha(f,t)} . \tag{5}$$

The difference of the squares the second and first moments will be equal to the variance. For a Gaussian shaped amplitude spectrum the variance is the square of the half bandwidth. In general variance is proportional the bandwidth. The second moment represents the instantaneous RMS frequency,

$$\sigma^2(t) = F^2_{RMS}(t) - F^2_{ave}(t) . \tag{6}$$

The bandwidth and RMS frequency measurements are instantaneous values and may contain local noise. First, we estimate the general trend with a weighted low pass filter of the variance (instead of actual bandwidth) and the RMS frequency; Since both the bandwidth and RMS frequency decay with time, we use their product rather than the individual term. Using the product of two observations is equivalent to the logical .AND. condition. The trend is computed by low pass filter and by weighting with the envelope. This will give more weight where there is high energy. We assume that the noise is in the background, generally in the relatively low amplitude zones. Let C(t) represent the product of RMS frequency and the bandwidth,

$$C(t) = 2.F_{RMS}(t).\sigma(t) . \tag{7}$$

The envelope weighted output, depending on the choice of filter W(t), is given by;

$$CW(t) = \frac{\sum_{T} E(t-\tau)C(t-\tau)W(\tau)}{\sum_{\tau} E(t-\tau)W(\tau)}. \qquad (8)$$

The local variation is also computed by envelope weighting, but with a relatively higher bandpass filtering; Let CL(t) and CS(t) represent low and high bandpass filtered outputs, respectively. Then the difference between the trend and the local variation is;

$$AZ(t) = CS(t) - CL(t). \qquad (9)$$

Here the zones to the left of the yellow line (negative values zones of AZ(t)) represent areas of lower frequency and narrower bandwidth, hence they can be interpreted as the anomalous absorption zone indicators.

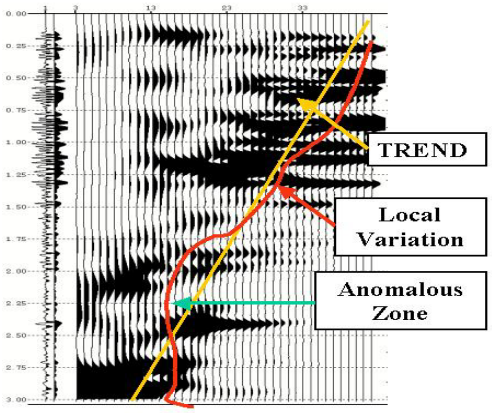

Figure 6: Gabor-Morlet decomposition of a seismic trace; Left most is the seismic trace, its envelope is plotted next to it. The middle group of traces represent the instantaneous amplitudes of the Gabor-Morlet sub-bands. The difference between the yellow trend line and the red local variation curve represents the possible anomalous zones.

Figure 6 schematically shows the joint time-frequency decomposition, given the general trend and the local variations.

Section 2 Conclusions

We have presented a simple method for the computation and detection of anomalous absorption zones. This zone indicator computation seems to be rather robust and can become a useful basis for several other computations. Since the actual Q computation is very noisy, it could be better to estimate Q values within anomalous absorption zones. A second use is to combine the anomalous absorption zone indicators with zones of low and high acoustic impedance. These hybrid attributes further focus our attention on the

possible areas of interest. For example low acoustic impedance with high absorption rates will indicate possible porous sands with gas. In carbonate zones we may look for high acoustic impedance with higher absorption rates.

References

Koehler, F., 1983, Gabor Wavelet Theory; SRC Internal report.

Morlet, J., Arens E., Fourgeau, E. and Giard D., 1982, Wave propagation and sampling theory-Part 1; Complex signal and scattering in multilayer media. Part I; Geophysics, v.47 no. 2, p. 203-221.

Morlet, J., Arens E., Fourgeau, E. and Giard D., 1982, Wave propagation and sampling theory-Part I1; Sampling theory and Complex waves. Part II; Geophysics.v.47 no. 2, p. 222-236. (* Discussion in GEO-49-09-1562-1563; Reply in GEO-49-09-1564-1564)

Taner, M. T. 1996, Q Computation and Compensation; RSI Technical report

Taner, M. T., Koehler. F. and Sheriff, R. E. , 1979, Complex Seismic Trace Analysis; Geophysics, 44, 1941-1063

Taner, M. T., 2001, Joint Time/Frequency Analysis, Q Quality Factor and Dispersion Computation Using Gabor-Morlet Wavelets or the Gabor-Morlet Transform; RSI Technical Report

Taner, M. T., Walls, J., Mavko, G., and Treitel, S., 2002, Q, Absorption and Dispersion computation by several different methods; RSI Technical Report.

Taner, M., T. 2001, Joint Time/Frequency Analysis, Q Quality Factor and Dispersion Computation Using Gabor-Morlet Wavelets or the Gabor-Morlet Transform; RSI Technical Report

Taner, M. T., Walls, J., Mavko, G., and Treitel, S., 2002, Q, Absorption and Dispersion computation by several different methods; RSI Technical Report.

Taner, M. T. , and Treitel, S., 2002, Q Computation and Compensation; RSI Q Project report.

Work Planned for Next Period

This report is for the final quarter of the project. All development work is complete and the final report is now being prepared.

Problems Encountered This Period

No significant problems have been encountered in our work during this period.